Spectrochimica Acta Part A: Molecular and Biomolecular Spectroscopy 106 (2013) 25–33

Contents lists available at SciVerse ScienceDirect

Spectrochimica Acta Part A: Molecular and Biomolecular Spectroscopy

journal homepage: www.elsevier.com/locate/saa

Investigations of FT-IR, FT-Raman, FT-NMR spectra and quantum chemical computations of Esculetin molecule

Yusuf Erdogdu *

Department of Physics, Ahi Evran University, 40040 Kirsehir, Turkey

HIGHLIGHTS

- FT-IR, FT-Raman and FT-NMR spectra of Esculetin molecule are recorded and analyzed.
- Theoretical approach to spectra based on DFT (B3LYP) method with 6-311++G(d,p), cc-pVDZ, cc-pVTZ and cc-pVQZ basis sets.
- The observed and calculated FT-IR, FT-Raman, ^{1}H and ^{13}C NMR chemical shifts are in close agreement.
- The most stable conformer has been predicted.
- All calculations are calculated theoretically using Gaussian 09 and Spartan 10 software.

GRAPHICAL ABSTRACT

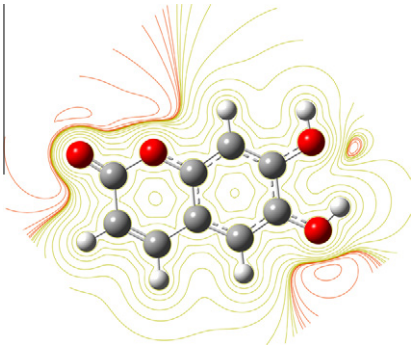

ARTICLE INFO

Article history:
Received 19 October 2012
Received in revised form 10 December 2012
Accepted 14 December 2012
Available online 23 December 2012

Keywords:
Esculetin
DFT
FT-IR
FT-Raman and FT-NMR

ABSTRACT

In this work, we report a combined experimental and theoretical study on molecular structure, vibrational spectra and electronic properties of Esculetin (ESC). The FT-IR, FT-Raman and FT-NMR spectra have been recorded and analyzed. The molecular geometry, harmonic vibrational frequencies, chemical shifts, HOMO, LUMO energies and molecular electrostatic potential map of ESC have been calculated by using Density Functional Theory (B3LYP) with 6-311G++(d,p), cc-pVDZ, cc-pVQZ and cc-pVTZ basis sets.

Introduction

Coumarin was first identified in 1820. It was first synthesized in the laboratory in 1868 [1]. Coumarins are of extensive current interests in chemical, biological, pharmacological. Coumarins are characterized by a wide spectrum of biological activity as for example the spasmolytic effect and antiarrhythmic, cardiothonic, antiviral, and anticancer properties [2–4]. Clinical studies reported antitumor activity of coumarin in several cancer types [5–7].

Experimental assays showed that coumarin is producing antiproliferative effect in tumor cell lines with mM concentrations. However, 7-hydroxycoumarin has greater antiproliferative activity [8–10]. The addition of two hydroxyl groups in the meta- or para-positions of the coumarin nucleus increases antiproliferative activity to ranges of μM concentration [11]. Dihydroxy-coumarin derivatives, Esculetin (6,7-dihydroxycoumarin) and daphnetin (7,8-dihydroxycoumarin), are secondary metabolites of plants used in folk medicine to counter inflammatory and allergic diseases [12,13]. Esculetin possesses diverse pleiotropic actions [14]: it inhibits smooth vascular muscle cell proliferation through the inhibition of kinases and mitogen signal pathways mediated

* Tel.: +90 03862528050; fax: +90 03862528054.
E-mail address: yusuferdogdu@gmail.com

1386-1425/$ - see front matter © 2012 Elsevier B.V. All rights reserved.
http://dx.doi.org/10.1016/j.saa.2012.12.043

by Ras protein [15]. The antiproliferative effect of Esculetin has been reported to be greater in tumor cells than in non-malignant cells [16–18]. Esculetin has been considered a promising anticancer agent due to its multiple properties [19].

Orozco et al. observed that the molecule produced biphasic effects, similar to those observed with other pythoestrogens in breast carcinoma MCF-7 cells. The inhibitory activity of Esculetin occurred only at μM concentrations. Meanwhile, lower concentrations produced estrogenic effects in vitro and in vivo that would limit its use as an anticancer agent in estrogen-dependent tumors [20].

In the present work, we report the results of FT-IR, FT-Raman and FT-NMR spectra, Molecular Orbital Energies, Non-linear optical properties and Molecular Electrostatic Potential of ESC molecule. The electronic and spectroscopic properties of this molecule have not yet been studied in detail to the best of our knowledge. Therefore, the present investigation was undertaken to study the structural, conformational, vibrational and electronic properties of the ESC molecule. Density Functional Theory (DFT/B3LYP) calculations have been performed to support our wavenumber assignments. Furthermore, we interpreted the calculated spectra in terms of total energy distributions (TEDs) and made the assignment of the experimental bands.

Experimental

The FT-IR spectrum of ESC molecule was recorded in the region 4000–400 cm^{-1} on IFS 66V spectrophotometer using KBr pellet technique. The FT-Raman spectrum of ESC molecule has been recorded using 1064 nm line of Nd: YAG laser as excitation wavelength in the region 50–3500 cm^{-1} on Bruker FRA 106/S. The ^{1}H and ^{13}C NMR spectra are taken in chloroform solutions and all signals are referenced to TMS on a Bruker Superconducting FT-NMR Spectrometer. All NMR spectra were measured at room temperature.

Computational details

The calculations were performed at DFT levels by using Gaussian 09 [21] program package, invoking gradient geometry optimization [21,22]. In order to establish the stable possible conformations, the conformational space of ESC molecule was scanned with molecular mechanic simulations. This calculation was performed with the Spartan 10 program [23]. In order to meet the requirements of both accuracy and computing economy, theoretical methods and basis sets should be considered. Density functional theory (DFT) has been proved to be extremely useful in treating electronic structure of molecules. The basis set 6-311++G(d,p) was used for the conformational analysis. The optimized structural parameters were used in the vibrational frequency calculations at the DFT level to characterize all stationary points as minima. Then, vibrationally averaged nuclear positions of ESC were used for harmonic vibrational frequency calculations resulting in IR and Raman frequencies together with intensities. In the present work, the DFT method B3LYP/6-311++G(d,p) were used for the computation of molecular structure, vibrational frequencies and energies of optimized structures. The vibrational modes were assigned on the basis of TED analysis for B3LYP/6-311++G(d,p), using SQM program [24].

It should be noted that Gaussian 09 package able to calculate the Raman activity. The Raman activities were transformed into Raman intensities using Raint program [25] by the expression:

$$I_i = 10^{-12} \times (v_0 - v_i)^4 \times \frac{1}{v_i} \times RA_i \quad (1)$$

where I_i is the Raman intensity, RA_i is the Raman scattering activities, v_i is the wavenumber of the normal modes and v_0 denotes the wavenumber of the excitation laser [26].

The ^{1}H and ^{13}C NMR chemical shifts calculations of the conformer 2 of the ESC molecule were made by using B3LYP functional with 6-311G++(d,p), cc-pVDZ, cc-pVQZ and cc-pVTZ basis sets. The GIAO (Gauge Including Atomic Orbital) method is one of the most common approaches for calculating isotropic nuclear magnetic shielding tensors [27,28]. Methods for computation of nuclear shielding at the SCF level using GIAO's enable reliable reproduction of chemical shifts for medium-size molecules [29]. The calculations are performed for an isolated molecule at its equilibrium geometry. The NMR spectra calculations were performed by Gaussian 09 program package. The calculations reported were performed in chloroform solution using IEF-PCM model as well as gas phase in agreement with experimental chemical shifts obtained in chloroform solution.

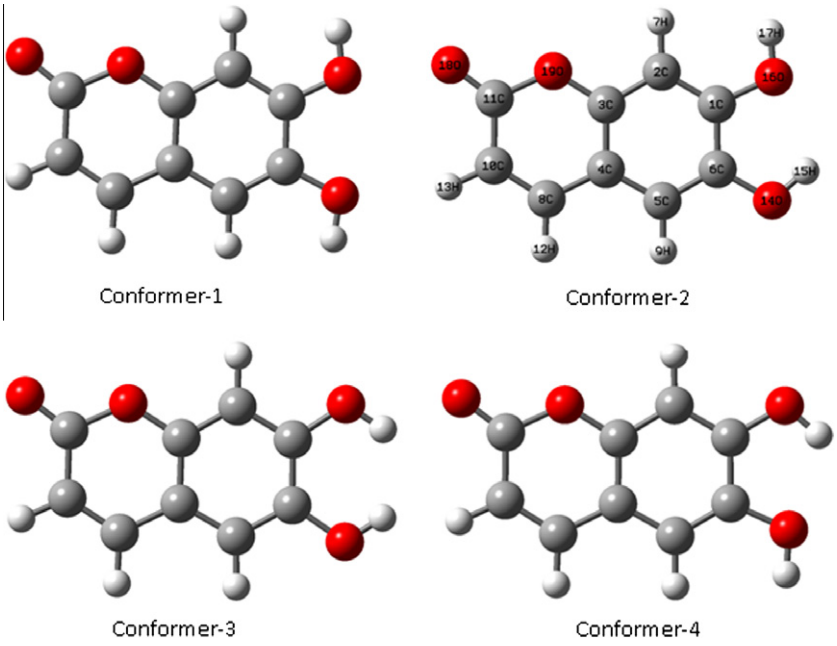

Fig. 1. All conformers structure of Esculetin molecule and atomic numbering.

Table 1
Energetic of the four conformers calculated at the B3LYP/6-311++G(d,p) level.

Conf.	E (Hartree)	ΔE (kcal/mol)	E_0 (Hartree)	ΔE_0 (kcal/mol)
1	−647.645653290	4.1601	−647.511350290	4.1369
2	−647.652282780	0.0000	−647.517942780	0.0000
3	−647.640450030	7.4252	−647.507664030	6.4500
4	−647.652141340	0.0888	−647.517791340	0.0950

E_0, Zero point corrected energy.

Results and discussion

Molecular geometry

The numbering scheme for ESC is shown in Fig. 1. Optimized bond parameters were calculated by using B3LYP with 6-311++G(d,p), cc-pVDZ, cc-PVTZ and cc-PVQZ basis sets. In order to find stable conformers, a meticulous conformational analysis was carried out for the title molecule. By rotating 10° intervals around the free rotation bonds, conformational space of the title

Table 2
Vibrational assignment of ESC by normal mode analysis based on SQM force field calculations.

Theoretical (B3LYP)							Experimental		TED[d] (%)
6-311++G(d.p)				cc-PVDZ	cc-PVTZ	cc-PVQZ	Exp. IR	Exp. Raman	
Normal modes	Freq[a]	I_{IR}[b]	I_{Raman}[c]	Freq[a]	Freq[a]	Freq[a]			
ν_1	77	0.452	2.368	82	80	80		82	$\Gamma_{CCCO}(27) + \Gamma_{CCCC}(17) + \Gamma_{CCOC}(17) + \Gamma_{CCCH}(14) + \Gamma_{OCCH}$ (10)
ν_2	112	0.547	5.124	116	115	115		107	$\Gamma_{CCCC}(31) + \Gamma_{CCCO}(22) + \Gamma_{CCCH}(16) + \Gamma_{CCOC}(13)$
ν_3	173	1.433	1.495	182	180	180			$\Gamma_{CCCC}(22)+\Gamma_{CCCO}(16) + \Gamma_{OCCH}(10) + \Gamma_{CCOC}(10)$
ν_4	206	20.98	9.275	236	236	237			$\Gamma_{COH}(64)+\Gamma_{CCC}(10)$
ν_5	236	0.487	3.265	263	261	261		224	$\delta_{CCO}(34) + \delta_{CCC}(26) + \nu_{CC}(16)$
ν_6	258	1.570	5.612	278	275	278			$\Gamma_{COH}(24)+\gamma_{CCO}(21) + \Gamma_{CCCC}(18) + \gamma_{COC}(14)$
ν_7	302	0.664	1.271	300	302	303			$\delta_{CCO}(50) + \delta_{CCC}(19) + \delta_{CCH}(10)$
ν_8	344	1.149	0.159	360	358	358			$\gamma_{COH}(52) + \gamma_{CCO}(17)$
ν_9	376	0.067	43.65	376	377	378			$\Gamma_{CCCC}(30) + \Gamma_{CCCO}(19) + \Gamma_{CCOH}(19) + \Gamma_{CCCH}(13)$
ν_{10}	379	5.861	1.681	405	402	408			$\delta_{CCC}(36) + \delta_{CCO}(23) + \delta_{CCH}(11) + \nu_{CO}(11)$
ν_{11}	405	0.141	33.00	417	406	409		406	$\delta_{CCC}(32) + \delta_{CCO}(25) + \nu_{CC}(12) + \delta_{CCH}(10)$
ν_{12}	412	0.224	7.927	429	424	425	413		$\Gamma_{CCCO}(21) + \Gamma_{CCOH}(15) + \Gamma_{OCCH}(14) + \Gamma_{CCCC}(12)$
ν_{13}	438	0.031	0.495	452	447	449	436	448	$\Gamma_{CCCC}(33) + \Gamma_{CCCH}(26)$
ν_{14}	481	0.706	8.246	480	482	485	482	508	$\delta_{CCC}(29) + \delta_{CCO}(27) + \delta_{CCH}(14)$
ν_{15}	553	6.336	6.394	553	554	557			$\delta_{CCO}(37) + \delta_{CCC}(21) + \delta_{CCH}(14)$
ν_{16}	589	0.023	1.378	589	590	593	582	573	δ_{CCC} (28) + $\delta_{CCO}(20) + \delta_{CCH}(17)$
ν_{17}	624	0.010	0.578	654	650	651	643	629	$\Gamma_{CCCC}(23) + \Gamma_{CCCH}(19) + \Gamma_{CCCO}(17) + \Gamma_{OCCH}(12)$
ν_{18}	659	2.913	1.578	661	661	663	662		$\delta_{CCC}(28) + \delta_{CCO}(23) + \nu_{CO}(11)$
ν_{19}	669	0.003	0.253	692	691	694	674		$\Gamma_{CCCC}(35) + \Gamma_{CCCH}(21) + \Gamma_{CCOH}(17)$
ν_{20}	708	0.195	0.718	736	739	743	722		$\Gamma_{CCH}(37) + \Gamma_{CCCC}(22) + \gamma_{CCO}(16) + \Gamma_{CCOC}(13)$
ν_{21}	738	0.965	45.41	743	740	743	747	759	$\nu_{CC}(30) + \delta_{CCC}(24) + \nu_{CO}(12) + \delta_{CCH}(11) + \delta_{CCO}(10)$
ν_{22}	781	0.034	0.751	788	783	786			$\nu_{CC}(28) + \nu_{CO}(24) + \delta_{CCC}(19) + \delta_{CCH}(11) + \delta_{CCO}(10)$
ν_{23}	796	4.410	0.098	814	815	816	809		$\gamma_{CCH}(71) + \Gamma_{CCCC}(15)$
ν_{24}	809	1.041	0.172	826	827	829	819	812	$\gamma_{CCH}(63) + \Gamma_{CCCC}(12)$
ν_{25}	837	0.922	1.851	837	841	845	846	835	$\gamma_{CCH}(72) + \Gamma_{CCCC}(11)$
ν_{26}	850	7.803	0.291	866	865	867			$\delta_{CCC}(35) + \delta_{CCH}(17) + \delta_{CCO}(14)$
ν_{27}	889	11.69	9.332	893	891	895	875	871	$\nu_{CC}(21) + \delta_{CCH}(24) + \nu_{CO}(18) + \delta_{CCO}(15)$
ν_{28}	964	0.076	1.792	981	982	986	944	948	$\gamma_{CCH}(63) + \Gamma_{OCCH}(15) + \Gamma_{CCCC}(10)$
ν_{29}	1051	8.439	26.47	1062	1056	1059			$\delta_{CCH}(31) + \nu_{CC}(21) + \nu_{CO}(17) + \delta_{CCC}(11)$
ν_{30}	1107	35.07	7.950	1121	1109	1112	1100		$\nu_{CO}(23) + \nu_{CC}(17) + \delta_{CCH}(16) + \delta_{COH}(16) + \delta_{CCC}(15)$
ν_{31}	1118	3.526	18.77	1125	1122	1126	1123	1115	$\delta_{CCH}(37) + \delta_{CCC}(17) + \nu_{CC}(13) + \delta_{COH}(11)$
ν_{32}	1155	3.069	19.97	1152	1158	1162	1149	1149	$\delta_{COH}(26) + \delta_{CCH}(24) + \nu_{CC}(19) + \nu_{CO}(10) + \delta_{CCC}(10)$
ν_{33}	1161	3.700	24.03	1162	1164	1168		1158	$\delta_{CCH}(52) + \nu_{CC}(14)$
ν_{34}	1184	3.172	2.205	1192	1188	1192	1195		$\delta_{CCH}(45) + \nu_{CC}(14) + \nu_{CO}(13)$
ν_{35}	1235	1.668	4.897	1235	1239	1243	1229	1224	$\delta_{CCH}(42) + \delta_{CCC}(20) + \nu_{CC}(12)$
ν_{36}	1266	54.98	17.22	1282	1266	1269	1270	1272	$\delta_{CCH}(34) + \nu_{CC}(17) + \delta_{CCC}(17) + \delta_{COH}(11)$
ν_{37}	1295	5.998	4.466	1318	1301	1304			$\delta_{CCH}(24) + \delta_{COH}(17) + \delta_{CCC}(16) + \nu_{CC}(14) + \nu_{CO}(13) + \delta_{CCO}(10)$
ν_{38}	1360	5.182	100	1374	1361	1363	1360		$\nu_{CC}(37) + \delta_{CCH}(15) + \delta_{COH}(14) + \delta_{CCO}(10)$
ν_{39}	1373	14.41	17.59	1391	1377	1382	1386	1396	$\delta_{CCH}(37) + \nu_{CC}(19) + \delta_{CCC}(11) + \delta_{CCO}(11)$
ν_{40}	1444	0.841	0.226	1462	1448	1452	1453	1438	$\delta_{CCH}(28) + \nu_{CC}(25) + \delta_{CCC}(13)$
ν_{41}	1489	14.95	5.944	1506	1492	1496	1482	1489	$\delta_{CCH}(32) + \nu_{CC}(27) + \nu_{CO}(10)$
ν_{42}	1555	34.70	91.88	1573	1555	1559	1558	1563	$\nu_{CC}(32) + \delta_{CCH}(22) + \delta_{CCO}(16) + \delta_{CCC}(11)$
ν_{43}	1608	0.691	14.02	1626	1609	1613	1605	1603	$\nu_{CC}(32) + \delta_{CCH}(20) + \delta_{CCC}(17)$
ν_{44}	1613	12.47	36.90	1636	1613	1617		1617	$\nu_{CC}(24) + \delta_{CCC}(17) + \delta_{CCH}(14) + \nu_{CO}(10)$
ν_{45}	1741	100	50.10	1777	1745	1745	1725	1672	$\nu_{CO}(25) + \nu_{CC}(21) + \delta_{CCO}(14)$
ν_{46}	3062	1.056	6.053	3081	3056	3066	3019		$\nu_{CH}(77)$
ν_{47}	3078	0.302	5.345	3097	3072	3082	3058	3053	$\nu_{CH}(77)$
ν_{48}	3085	0.325	9.108	3104	3079	3088		3073	$\nu_{CH}(75)$
ν_{49}	3110	0.032	11.46	3128	3106	3115	3144	3092	$\nu_{CH}(78)$
ν_{50}	3670	17.22	3.547	3631	3651	3669	3629		$\nu_{OH}(91)$
ν_{51}	3716	15.72	5.859	3677	3693	3709			$\nu_{OH}(92)$

vs: Very strong; ms: medium strong; s: strong; w: weak; vw: very weak; ν: stretching; t: torsion; γ: out of plane stretching; δ: in plane bending.
[a] Obtained from the wave numbers calculated at 0.967 for 6-311++G(d,p)), 0.970 for cc-pVDZ, 0.965 for cc-pVTZ 0.969 for cc-pVQZ.
[b,c] Relative absorption intensities and Relative Raman intensities normalized with highest peak absorption equal to 100.
[d] Total energy distribution calculated B3LYP/6-311++G(d,p) level of theory. Only contributions $\geqslant$10% are listed.

molecule was scanned by molecular mechanic simulations and then full geometry optimizations of these structures were performed by B3LYP/6-311++G(d,p) method. Results of geometry optimizations indicated that the ESC molecule is rather flexible molecule and, in theory, may have at least four conformers as shown in Fig. 1. Ground state energies, zero point corrected energies (E_{elect} + ZPE), relative energies and dipole moments of conformers were presented in Table 1. Zero point corrections have not caused any significant changes in the stability order. Optimized geometric parameters listed in Table S1.

Vibrational assignments

The molecule ESC consist of 19 atoms, hence has 51 normal modes of vibrations. The harmonic wavenumber calculations were performed with B3LYP/6-311++G(d,p), cc-pVDZ, cc-PVTZ and cc-PVQZ basis sets. The title molecule belongs to C_1 point group symmetry. All vibrations are active in both Raman and infrared spectroscopy. The recorded FT-IR, FT-Raman and calculated wavenumbers and intensities (IR, Raman) are given in Table 2. The experimental spectra are shown in Fig. 2 (FT-IR), and Fig. 3 (FT-Raman). The total energy distributions for all fundamental vibrations were calculated using scaled quantum mechanics (SQMs) method at B3LYP/6-311++G(d,p) level.

O—H vibrations

The non-hydrogen bonded or free hydroxyl group absorbs strongly in the 3700–3584 cm^{-1} region while the existence of intermolecular hydrogen bond formation can lower the O—H stretching wavenumber to the 3550–3200 cm^{-1} region [30,31]. The O—H vibrations are extremely sensitive to formation of hydrogen bonding [30,31]. In the present investigation, the O—H stretching band is recorded at 3629 cm^{-1} using FT-IR whereas there is no Raman counterpart. The DFT computations give the wavenumber of this band at 3670 and 3716 cm^{-1} (mode nos: 50 and 51) for the O—H stretch vibrations. The TED values >90% support the present assignments.

The O—H in-plane bending vibrations, in general, lies in the region 1150–1250 cm^{-1} and is not much affected due to hydrogen bonding unlike to stretching and out-of-plane bending wavenumbers [32]. In the present work, the O—H in-plane bending modes observed at 1100 cm^{-1} (30 mode number), 1149 cm^{-1} (32 mode number) in FT-IR and 1149 cm^{-1} (32 mode number) in FT-Raman spectra. In plane vibrations of OH are predicted at 1107 cm^{-1} (30 mode number), 1155 cm^{-1} (32 mode number) and 1295 cm^{-1} (37 mode number) for B3LYP/6-311++G(d,p) level of theory. DFT calculation shows that the OH in-plane bending vibrations are mixed with the C—C—H bending and C—C stretching vibrations. The O—H out-of-plane deformation vibration for phenol lies in the region 290–320 cm^{-1} for free OH [33]. Out-of-plane bending mode of OH group predict at 206 cm^{-1}, 258 cm^{-1} and 344 cm^{-1} (Mode nos: 4, 6 and 8/B3LYP/6-311++G(d,p)).

C—H vibrations

The heteroaromatic structure shows that the presence of the C—H stretching vibration in the range 3000–3100 cm^{-1} which is the characteristic region for the ready identification of C—H stretching vibration [34]. In ESC molecule, the carbon bonded hydrogen atom stretching vibrations are observed at 3019, 3058 and 3144 cm^{-1} as medium strong band in FT-IR and 3053, 3073 and 3092 cm^{-1} (medium) in FT-Raman. The computed wavenumbers for the same mode are assigned in the range of 3110–3062 cm^{-1}/B3LYP/6-311++G(d,p)/mode nos: 46–49. In which mode nos: 46 (C_5-H_9), 47 (C_8-H_{12}), 48 (C_2-H_7) and 49 (C_{10}-C_{13}) are belongs to C—H stretching vibrations in rings.

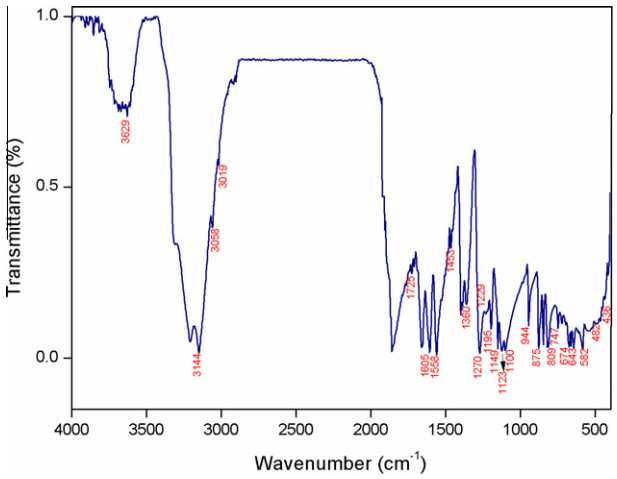

Fig. 2. Experimental FT-IR spectra of Esculetin molecule.

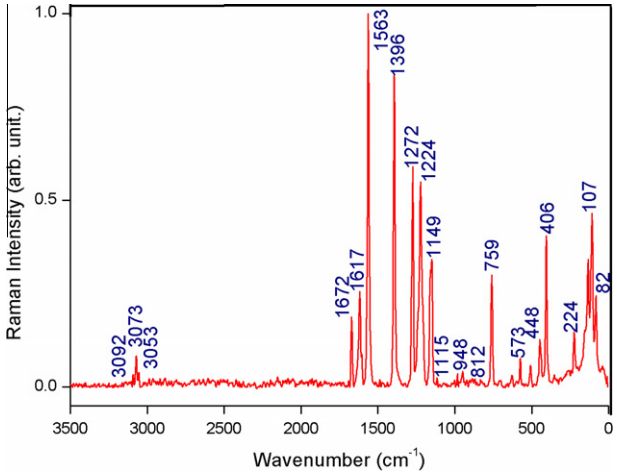

Fig. 3. The experimental FT-Raman spectra of Esculetin molecule.

Table 3
Theoretical and experimental ^1H and ^{13}C spectra of the conformer-2 of ESC molecule (with respect to TMS, all values in ppm).

	B3LYP (Theoretical)				Experimental	
	6-311++G(d.p)	cc-pVDZ	cc-pVTZ	cc-pVQZ	New exp.	Exp.[a]
C_{11}	164.47	145.23	163.77	169.303	162.63	160.4
C_3	156.93	139.43	155.84	161.099		148.1
C_1	152.47	135.92	152.47	157.518	145.61	150.2
C_8	150.06	133.13	148.71	154.593	144.28	143.5
C_6	147.93	131.12	146.84	152.035	138.42	142.7
C_4	118.67	103.99	117.11	122.422	109.30	112.4
C_5	116.51	102.24	114.88	120.106	107.89	114.2
C_{10}	116.50	100.82	114.77	120.039	105.46	112.3
C_2	105.00	90.796	103.34	108.310	101.04	104.4
H_{12}	7.753	7.820	8.016	8.158	10.00	
H_9	7.017	7.135	7.308	7.453	9.50	
H_7	6.774	6.927	7.012	7.127	7.893	
H_{13}	6.118	6.360	6.382	6.521	7.021	
H_{15}	5.188	5.195	5.642	5.796	6.790	
H_{17}	4.789	4.690	5.147	5.399	6.201	

[a] Taken from Ref. [45].

The C—H in-plane bending vibrations appear in the region 1300–1000 cm^{-1} and C—H out of plane bending vibrations in the range of 1000–750 cm^{-1}. The bands corresponding to the C—H in-plane bending vibrations identified in ESC at 1123 cm^{-1},

Table 4
Dipol moment, Polarizability and Hyperpolarizability of Esculetin molecule for B3LYP with 6-311++G(d,p), cc-pVDZ, cc-pVTZ and cc-pVQZ basis sets.

	Dipol Moment	Polarizability	Hyperpolarizability		Dipol Moment	Polarizability	Hyperpolarizability				
B3LYP/6-311++G(d.p)	μ 1.662	α_{AVE}	125.61	β_{xxx}	−846.354	cc-pVTZ	μ 1.705	α_{AVE}	120.45	β_{xxx}	−737.106
		Δα	70.222	β_{xxx}	293.202			Δα	72.692	β_{xxx}	229.588
				β_{xxx}	−83.465					β_{xxx}	−59.572
				β_{xxx}	79.503					β_{xxx}	3.494
				β_{xxx}	0.000					β_{xxx}	0.000
				β_{xxx}	0.000					β_{xxx}	0.000
				β_{xxx}	0.000					β_{xxx}	0.000
				β_{xxx}	−34.745					β_{xxx}	−10.192
				β_{xxx}	−15.612					β_{xxx}	−4.546
				β_{xxx}	0.000					β_{xxx}	0.000
				β	1028.544					β	838.61
B3LYP/cc-pVDZ	μ 1.693	α_{AVE}	112.16	β_{xxx}	−743.535	B3LYP/cc-pVQZ	μ 1.705	α_{AVE}	125.41	β_{xxx}	−747.860
		Δα	77.758	β_{xxx}	225.716			Δα	70.652	β_{xxx}	242.847
				β_{xxx}	−50.038					β_{xxx}	−70.966
				$\beta_{xxx;}$	−7.922					β_{xxx}	24.921
				β_{xxx}	0.000					β_{xxx}	0.000
				β_{xxx}	0.000					β_{xxx}	0.000
				β_{xxx}	0.000					β_{xxx}	0.000
				β_{xxx}	−2.161					β_{xxx}	−16.568
				β_{xxx}	−3.026					β_{xxx}	−9.651
				β_{xxx}	0.000					β_{xxx}	0.000
				β	824.20					β	874.362

1195 cm^{-1}, 1229 cm^{-1}, 1270 cm^{-1}, in FT-IR spectra and 1115 cm^{-1}, 1158 cm^{-1}, 1224 cm^{-1} and 1272 cm^{-1} in FT-Raman spectra. The corresponding calculated modes are dominated by C—H in plane bending and coupled with CC and CO stretching. Out-of-plane bending vibrations are observed at 722 cm^{-1} (708 cm^{-1} for DFT), 809 cm^{-1} (796 cm^{-1} for DFT), 819 cm^{-1} (812 cm^{-1} for FT-Raman and 809 cm^{-1} for DFT), 846 cm^{-1} (835 cm^{-1} for FT-Raman and 837 cm^{-1} for DFT) and 944 cm^{-1} (948 cm^{-1} for FT-Raman and 964 cm^{-1} for DFT) in the FT-IR spectra. These assignments are in the expected range and also find support from literature [35,36].

CO vibrations

The carbonyl stretching frequency has been most extensively studied by infrared spectroscopy [37]. This multiply bonded group is highly polar and therefore gives rise to an intense infrared absorption band. The carbon–oxygen double bond is formed by p_π–p_π bonding between carbon and oxygen. Because of the different electro negativities of carbon and oxygen atoms, the bonding electrons are not equally distributed between the two atoms. The following two resonance forms contribute to the bonding of the carbonyl group >C═O ↔ C^+—O^-. The lone pair of electrons on oxygen also determines the nature of the carbonyl group. The carbonyl stretching vibrations are found in the region 1780–1700 cm^{-1} [38]. In ESC, the band appeared at 1725 cm^{-1} (FT-IR) and 1672 cm^{-1} (FT-Raman) is belongs to C═O group. The corresponding calculated wavenumber is at 1741 cm^{-1} (mode no.: 40) using B3LYP/ 6-311++G(d,p) basis set.

CC vibrations

Generally the CC stretching vibrations in aromatic compounds are seen in the region of 1430–1650 cm^{-1}. In our present study, the CC stretching vibrations observed at 1605 cm^{-1} (1603 cm^{-1} FT-Raman), 1558 cm^{-1} (1563 cm^{-1} FT-Raman) and 1360 cm^{-1} in FT-IR spectra. 1617 cm^{-1} in the FT-Raman spectra mode is assigned to the CC stretching vibrations. This mode is not observed at FT-IR spectra. As it evident from Table 2, the modes no.: 38, 42, 43 and 44 (B3LYP/6-311++G(d,p)) are in agreement with experimental observation and also find support from literature [39–43].

NMR spectra

Theoretical and experimental ^1H and ^{13}C spectra of the conformer-2 of ESC molecule are given in Table 3. The isotropic chemical shifts are frequently used as an aid in identification of reactive ionic species. It is recognized that accurate predictions of molecular geometries are essential for reliable calculations of magnetic properties. The NMR spectra calculations were performed for chloroform solvent. It is necessary to consider the solvent effects because the spectral data available are obtained in different solutions. The isotropic shielding values were used to calculate the isotropic chemical shifts δ with respect to tetramethylsilane (TMS) ($\delta_{iso}^X = \sigma_{iso}^{TMS} - \sigma_{iso}^X$).

The predicted and measured ^1H NMR spectrum of ESC revealed six signals in the aromatic region. Four of these signals were

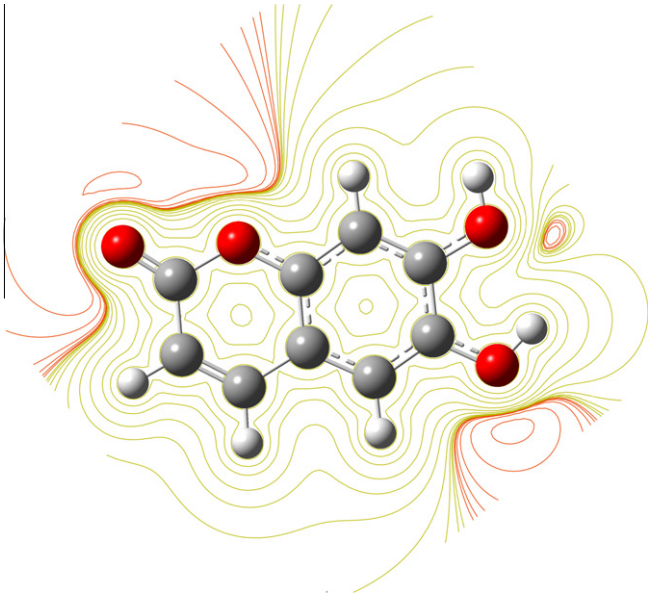

Fig. 4. Molecular electrostatic potential map (a).

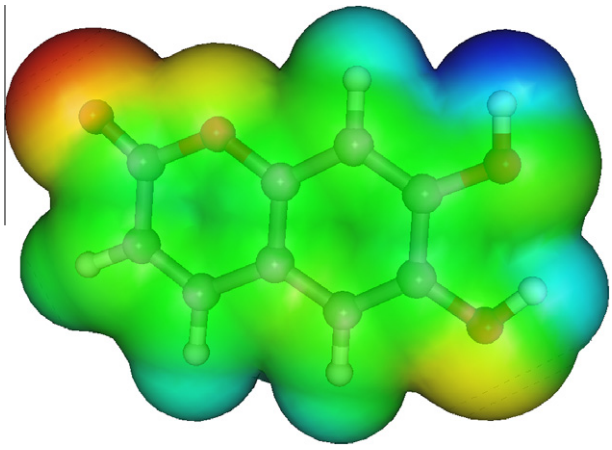

Fig. 5. Molecular electrostatic potential map (b).

assigned to the coumarin moiety. In ^{1}H NMR spectra of ESC molecule, these peaks observed in the interval 7.021–10.0 ppm for the H atoms of coumarins ring. The other two signals were assigned to the hydroxyl group. The peaks of H atoms of hydroxyl group are slightly smaller than those of coumarins ring. ^{1}H NMR peaks of hydroxyl group are experimentally observed at 6.201(H_{17}) ppm and 6.790 (H_{15}) ppm. The calculated chemical shift values for the hydroxyl proton were 5.796 (H_{15}) ppm and 5.399 (H_{17}) ppm for B3LYP/cc-pVQZ level of theory.

The ^{13}C NMR spectroscopy of coumarins and their derivatives was reviewed by Mikhova and Duddeck [44]. Zolek et al. [45] reported that the ^{13}C CP MAS NMR spectra were experimental recorded for a series of 11 solid coumarins with $CDCl_3$ solution. The ^{13}C chemical shifts of these compounds were determined by Zolek et al. [45]. Chemical shifts of Carbon-11 were observed at 160.4 ppm by Zolek. In this study, the signal at 162.63 ppm was assigned to the C_{11} carbon. The ^{13}C NMR data for ESC were also compared to their corresponding calculated values. This peak was calculated at 169.303 ppm for B3LYP/cc-pVQZ level of theory.

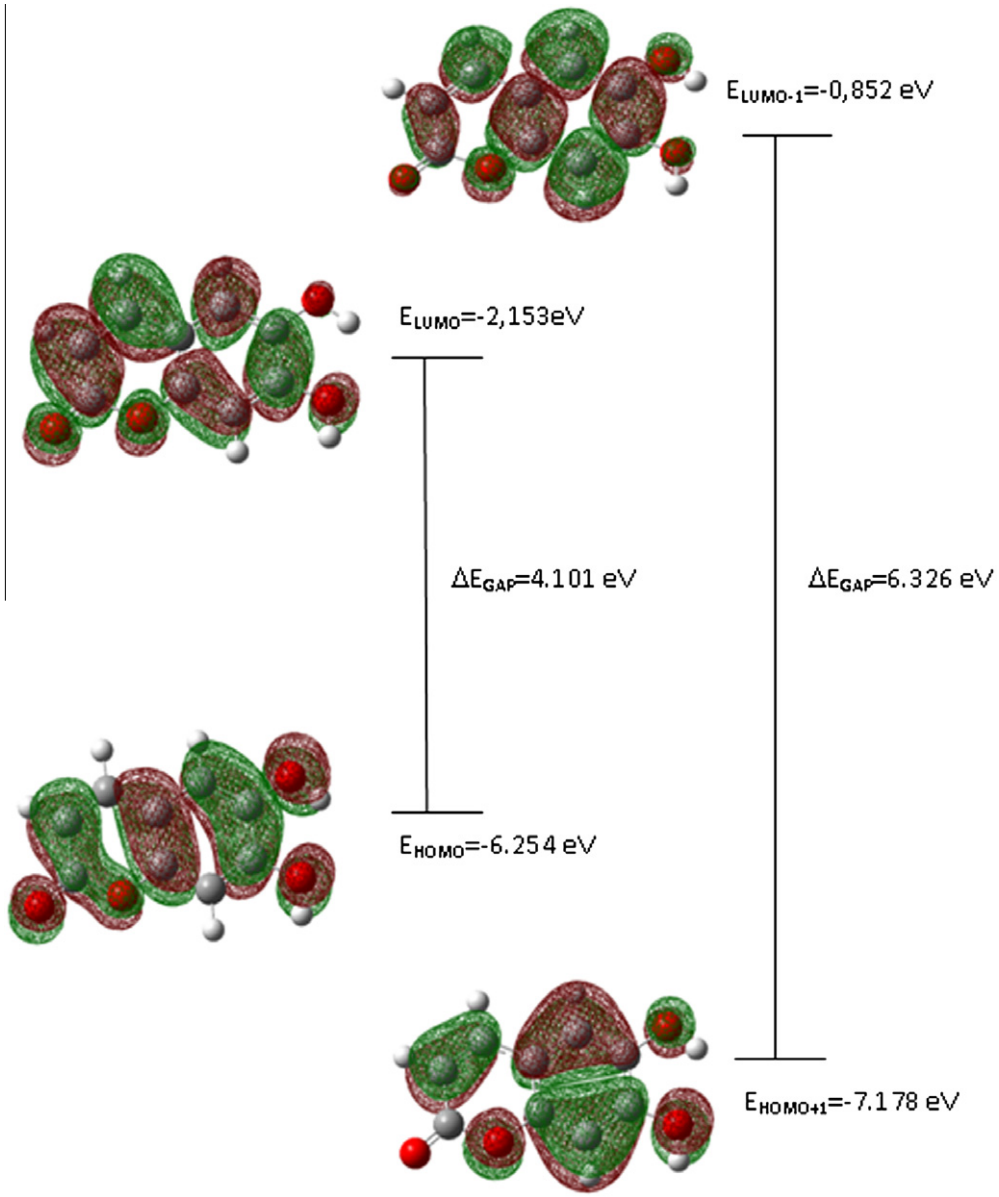

Fig. 6. The atomic orbital compositions of the frontier orbitals of Esculetin molecule.

The range of the ^{13}C NMR chemical shifts for a typical organic molecule usually is >100 ppm [46–48] and the accuracy ensures reliable interpretation of spectroscopic parameters. In the present paper, the ^{13}C NMR chemical shifts for the title molecule are >100 ppm, as they were expected. In the ^{13}C NMR, two signals at 145.61 ppm and 138.42 is due to C_1 and C_6 carbons respectively. The aromatic carbons in this compound are resonated at 125.75 ppm and 124.21 ppm. These carbon atoms are attached to the hydroxyl groups. The theoretically generated ^1H NMR and ^{13}C NMR spectra correlate well with the experimental spectra.

Hyperpolarizability calculation

The first hyperpolarizabilities (β_0, α_0 and $\Delta\alpha$) of ESC is calculated using B3LYP/6-311++G(d,p) basis set, based on the finite-field approach. In the presence of an applied electric field, the energy of a system is a function of the electric field. First hyperpolarizability is a third rank tensor that can be described by a $3 \times 3 \times 3$ matrix. The 27 components of the 3D matrix can be reduced to 10 components due to Kleinman symmetry [49]. It can be given in the lower tetrahedral format. It is obvious that the lower part of the $3 \times 3 \times 3$ matrix is a tetrahedral. The components of β are defined as the coefficients in the Taylor series expansion of the energy in the external electric field. When the external electric field is weak and homogeneous, this expansion becomes:

$$E = E^0 - \mu_\alpha F_\alpha - 1/2\alpha_{\alpha\beta}F_\alpha F_\beta - 1/6\beta_{\alpha\beta\gamma}F_\alpha F_\beta F_\gamma \quad (2)$$

where E^0 is the energy of the unperturbed molecules, F_α the field at the origin, and μ_α, $\alpha_{\alpha\beta}$, $\beta_{\alpha\beta\gamma}$ are the components of the dipole moment, polarizability and the first hyperpolarizabilities, respectively. The total static dipole moment μ, the mean polarizability α_0, the anisotropy of polarizability $\Delta\alpha$ and the mean first hyperpolarizability β_0, using the x, y, z components are defined as:

$$\mu = (\mu_x^2 + \mu_y^2 + \mu_z^2) \quad (3)$$

$$\alpha_0 = \frac{\alpha_{xx} + \alpha_{yy} + \alpha_{zz}}{3} \quad (4)$$

$$\Delta\alpha = 2^{1/2}[(\alpha_{xx} - \alpha_{yy})^2 + (\alpha_{yy} - zz)^2 + (\alpha_{zz} - \alpha_{xx})^2 + 6(\alpha_{xy}^2 + \alpha_{yz}^2 + \alpha_{yz}^2)]^2 \quad (5)$$

$$\beta_0 = (\beta_x^2 + \beta_y^2 + \beta_z^2)^{1/2} \quad (6)$$

$$\beta_x = \beta_{xxx} + \beta_{xyy} + \beta_{xzz} \quad (7a)$$

$$\beta_y = \beta_{yyy} + \beta_{xxy} + \beta_{yzz} \quad (7b)$$

$$\beta_z = \beta_{zzz} + \beta_{xxz} + \beta_{yyz} \quad (7c)$$

The total molecular dipole moment (μ) are 1.662 D (for 6-311++G(d,p) basis set), 1.693 D (for cc-pVDZ basis set), 1.705 D (for cc-pVTZ and cc-pVQZ basis sets) using B3LYP level of theory. The mean first hyperpolarizability (β_0) are 8.885×10^{-30} esu (for 6-311++G(d,p) basis set), 7.120×10^{-30} esu (for cc-pVDZ basis set), 7.245×10^{-30} esu (for cc-pVTZ basis set) and 7.553×10^{-30} esu (for cc-pVQZ basis set) by using B3LYP level of theory. The electric dipole moment, polarizability and hyperpolarizability of *ESC* are shown in Table 4. The similar parameters were calculated for earlier works [50,51].

Molecular electrostatic potential maps

The molecular electrostatic potential (ESP) at a point r in the space around a molecule is (in atomic units).

$$V(r) = \sum_A \frac{Z_A}{|R_A - r|} - \int \frac{\rho(r)dr'}{|r' - r|} \quad (8)$$

Z_A is the charge on nucleus A located at R_A and $\rho(r)$ is the electron density. The first term in the expression represents the effect of the nuclei and the second represents that of electrons. The two terms have opposite signs and therefore opposite effects. $V(r)$ is

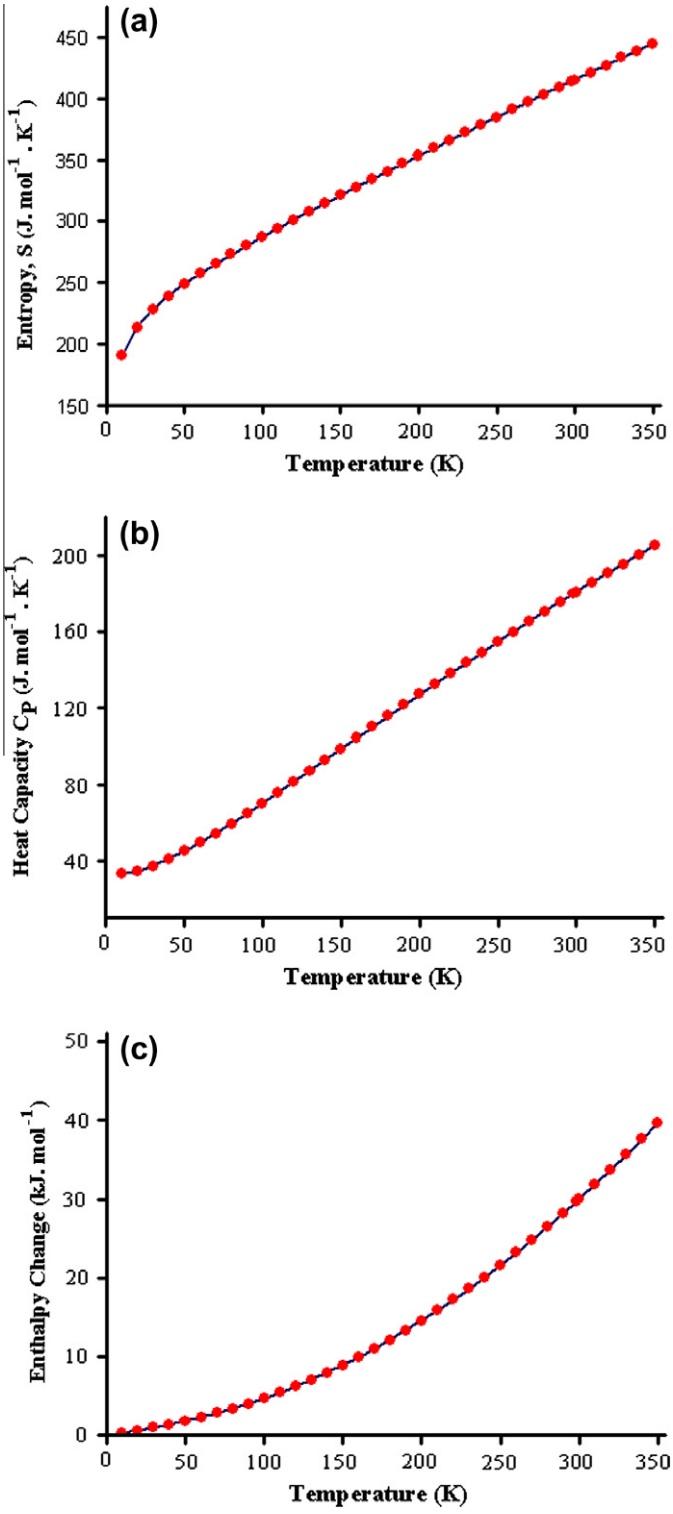

Fig. 7. Effect of temperature on entropy (a) heat capacity at constant pressure (C_p), (b) and enthapy change ($\Delta H_{o\rightarrow T}$) and (c) of Esculetin compound.

their resultant at each point r; it is an indication of the net electrostatic effect produced at the point r by the total charge distribution (electrons + nuclei) of the molecule.

The molecular electrostatic potential (MESP) is the most useful electrostatic property to study the relation between structure and activity. The MESP has been also employed as an informative tool of chemistry to describe different physical and chemical features, including non-covalent interactions in complex biological system. The molecular electrostatic potential maps of ESC are shown in Figs. 4 and 5.

HOMO–LUMO analysis

The atomic orbital compositions of the frontier molecular orbitals of ESC are shown in Fig. 6. The HOMO–LUMO energy gap of these compounds was calculated at the B3LYP/6-311++(d,p) level. The HOMO represents the ability to donate an electron, LUMO as an electron acceptor represents the ability to obtain an electron.

Several important molecular properties such as chemical hardness (η) and electronegativity (χ) have been defined based on quantum chemical calculations [52–54]. According to the Koopman theorem [55], Chemical hardness (η), and electronegativity (χ) are defined in the following equations:

$$\chi \cong -1/2(E_{\mathrm{HOMO}} + E_{\mathrm{LUMO}}) \quad (9)$$

$$\eta \cong -1/2(E_{\mathrm{HOMO}} - E_{\mathrm{LUMO}}) \quad (10)$$

Chemical hardness has been used as a tool to understand the chemical reactivity and some other properties of a molecular system [56]. Zhou and Parr [57] reported that stability of molecules is related to its chemical hardness. The concept of electronegativity has been introduced as the power of an atom in a molecule to attract electrons onto itself [58]. As a result, when the gap is large (other things being equal), one expects high stability and low reactivity. When it is small, one expects low stability and high reactivity [59].

Thermodynamic analysis

The temperature dependence of the thermodynamic properties heat capacity at constant pressure (C_p), entropy (S) and enthalpy change ($\Delta H_{0\rightarrow T}$) for Esculetin were also determined by B3LYP/6-311++G(d,p) method and listed in Table S2. The Fig. 7 depicts the correlation of heat capacity at constant pressure (C_p), entropy (S) and enthalpy change ($\Delta H_{0\rightarrow T}$) with temperature. The entropies, heat capacities, and enthalpy changes are increasing with temperature ranging from 10 to 350 K.

Conclusion

FT-IR, FT-Raman and FT-NMR spectra of the ESC have been recorded and analyzed. The gas phase structure and conformational properties of ESC and its conformers were determined by quantum chemical calculations. It is found that molecule has four conformations. Complete vibrational analysis of the most stable conformer of ESC was performed according to the SQM force field method based on DFT calculations at B3LYP/6-311++G(d,p) level.

Acknowledgement

Y. Erdogdu would like to thank Ahi Evran University Research Fund for its financial support, Project Numbers: FEN.4003.12.013. Computing resources used in this work were provided by the National Center for High Performance Computing of Turkey (UYBHM).

Appendix A. Supplementary material

Supplementary data associated with this article can be found, in the online version, at http://dx.doi.org/10.1016/j.saa.2012.12.043.

References

[1] N.I. Sax, Dangerous Properties of Industrial Materials, fourth ed., Van Nostrand Co., New York, 1975.
[2] M. Gabor, The Pharmacology of Benzopyrone Derivatives and Related Compounds, Akademiai Kiado, Budapest, 1988. pp. 91–126.
[3] E. Budzisz, Phosph. Sulf. Silicon Relat. Elem. 179 (2004) 2131.
[4] F. Borges, F. Roleira, N. Milhazes, L. Santana, E. Uriarte, Curr. Med. Chem. 12 (2005) 887.
[5] M.E. Marshall, K. Butler, A. Fried, Mol. Biother. 3 (1991) 170–178.
[6] J.L. Mohler, L.G. Gomella, E.D. Crawford, L.M. Glode, C.D. Zippe, W.R. Fair, M.E. Marshall, Prostate 20 (1992) 123–131.
[7] R.D. Thornes, L. Daly, G. Lynch, B. Breslin, H. Browne, H.Y. Browne, T. Corrigan, P. Daly, G. Edwards, E. Gaffney, J. Henley, T. Henley, F. Keana, F. Lennon, N. McMurray, S. O'Loughlin, M. Shine, A. Tanner, J. Cancer Res. Clin. Oncol. 120 (1994) 32–34.
[8] F.A. Jiménez-Orozco, J.A. Molina-Guarneros, N. Mendoza-Patiño, B. Flores-Pérez, F. León-Cedeño, E. Santos-Santos, J.J. Mandoki, Melanoma Res. 9 (1999) 243–247.
[9] F.A. Jiménez-Orozco, J.S. Lopez, A. Nieto, J. Molina, M.A. Velasco, N. Mendoza, M.J. García, P. Elizalde, F. León, J.J. Mandoki, Lung Cancer 34 (2001) 185–194.
[10] J.S. Lopez-Gonzalez, H. Prado-Garcia, D. Aguilar-Cazares, J.A. Molina-Guarneros, J. Morales-Fuentes, J.J. Mandoki, Lung Cancer 43 (2004) 275–283.
[11] H. Kolodziej, O. Kayser, H.J. Woerdenbag, W. van Uden, N. Pras, Z. Naturforsch. C. 52 (1997) 240–244.
[12] K.C. Fylaktakidou, D.J. Hadjipavlou-Litina, K.E. Litinas, D.N. Nicolaides, Curr. Pharm. Des. 10 (2004) 3813–3833.
[13] M.E. Riveiro, N. De Kimpe, A. Moglioni, R. Vázquez, F. Monczor, C. Shayo, C. Davio, Curr. Med. Chem. 17 (2010) 1325–1338.
[14] C.Y. Chu, Y.Y. Tsai, C.J. Wang, W.L. Lin, T.H. Tseng, Eur. J. Pharmacol. 416 (2001) 25–32.
[15] S.L. Pan, Y.W. Huang, J.H. Guh, Y.L. Chang, C.Y. Peng, C.M. Teng, Biochem. Pharmacol. 65 (2003) 1897–1905.
[16] G.J. Finn, E. Kenealy, B.S. Creaven, D.A. Egan, Cancer Lett. 183 (2002) 61–68.
[17] S. Kawaii, Y. Tomono, K. Ogawa, M. Sugiura, M. Yano, Y. Yoshizawa, Anticancer. Res. 21 (2001) 917–924.
[18] M. Kawase, H. Sakagami, K. Hashimoto, S. Tani, H. Hauer, S.S. Chatterjee, Anticancer. Res. 23 (2003) 3243–3246.
[19] A. Lacy, R. O'Kennedy, Curr. Pharma. Des. 10 (2004) 3797–3811.
[20] F.A.J. Orozco, A.A.R. Rosales, A.V. López, M.L.D. López, M.J.G. Mondragón, A.M. Espinoza, C. Lemini, N.M. Patiño, J.J. Mandoki, Eur. J. Pharmacol. 668 (2011) 35–41.
[21] M.J. Frisch, G.W. Trucks, H.B. Schlegel, G.E. Scuseria, M.A. Robb, J.R. Cheeseman, G. Scalmani, V. Barone, B. Mennucci, G.A. Petersson, H. Nakatsuji, M. Caricato, X. Li, H.P. Hratchian, A.F. Izmaylov, J. Bloino, G. Zheng, J.L. Sonnenberg, M. Hada, M. Ehara, K. Toyota, R. Fukuda, J. Hasegawa, M. Ishida, T. Nakajima, Y. Honda, O. Kitao, H. Nakai, T. Vreven, J.A. Montgomery, Jr., J.E. Peralta, F. Ogliaro, M. Bearpark, J.J. Heyd, E. Brothers, K.N. Kudin, V.N. Staroverov, R. Kobayashi, J. Normand, K. Raghavachari, A. Rendell, J.C. Burant, S.S. Iyengar, J. Tomasi, M. Cossi, N. Rega, J.M. Millam, M. Klene, J.E. Knox, J.B. Cross, V. Bakken, C. Adamo, J. Jaramillo, R. Gomperts, R.E. Stratmann, O. Yazyev, A.J. Austin, R. Cammi, C. Pomelli, J.W. Ochterski, R.L. Martin, K. Morokuma, V.G. Zakrzewski, G.A. Voth, P. Salvador, J.J. Dannenberg, S. Dapprich, A.D. Daniels, O. Farkas, J.B. Foresman, J.V. Ortiz, J. Cioslowski, D.J. Fox, Gaussian 09, Revision A.02, Gaussian, Inc., Wallingford CT, 2009.
[22] H.B. Schlegel, J. Comput. Chem. 3 (1982) 214–218.
[23] Spartan 10, Wavefunction Inc., Irvine, CA 92612, USA, 2010.
[24] G. Rauhut, P. Pulay, J. Phys. Chem. 99 (1995) 3093.
[25] D. Michalska, Raint Program, Wroclaw University of Technology, 2003.
[26] D. Michalska, R. Wysokinski, Chem. Phys. Lett. 403 (2005) 211–217.
[27] R. Ditchfield, J. Chem. Phys. 56 (1972) 5688.
[28] K. Wolinski, J.F. Hinton, P. Pulay, J. Am. Chem. Soc. 112 (1990) 8251–8260.
[29] C.J. Jameson, A.C. de Dios, Nucl. Magn. Reson. 28 (1999) 42.
[30] D. Sajan, Y. Erdogdu, T. Kuruvilla, I.H. Joe, J. Mol. Struct. 983 (2010) 12–21.
[31] Y. Erdogdu, M. Drozd, M.K. Marchewka, Vib. Spectrosc. 58 (2012) 169–180.
[32] G. Varsanyi, Assignments for Vibrational Spectra of Seven Hundred Benzene Derivatives, vols. 1 and 2, Academiai Kiado, Budapest, 1973.
[33] D. Michalska, D.C. Bienko, A.J.A. Bienko, Z. Latajka, J. Phys. Chem. 100 (1996) 17786.
[34] H. Saleem, Y. Erdogdu, S. Subashchandrabose, Ö. Dereli, V. Thanikachalam, J. Jayabharathi, Spectrochim. Acta Part A 86 (2012) 231–241.
[35] V. Thanikachalam, V. Periyanayagasamy, J. Jayabharathi, G. Manikandan, H. Saleem, S. Subashchandrabose, Y. Erdogdu, Spectrochim. Acta Part A 58 (2012) 169–180.
[36] H. Saleem, Akhil R. Krishnan, Y. Erdogdu, S. Subashchandrabose, V. Thanikachalam, G. Manikandan, J. Mol. Struct. 999 (2011) 2–9.
[37] G. Socrates, Infrared and Raman characteristic Group Frequencies Tables and Charts, third ed., Wiley, New York, 2001.

[38] D. Sajan, Y. Erdogdu, R. Reshmy, Ö. Dereli, K. Kurien Thomas, I. Hubert Joe, Spectrochim. Acta Part A 82 (2011) 118–125.
[39] V. Krishna kumar, R. John Xavier, Ind. J. Pure Appl. Phys. 41 (2003) 5–99.
[40] D.N. Sathyanarayana, Vibrational Spectroscopy Theory and Applications, second ed., New Age International (P) Limited Publisher, New Delhi, 2004.
[41] P.S. Kalsi, Spectroscopy of Organic Compounds, Wiley Eastern Ltd., New Delhi, 1993. pp. 117–118.
[42] R.L. Peesole, L.D. Shield, I.C. Mcwillam, Modern Methods of Chemical Analysis, Wiley, New York, 1976.
[43] A.R. Prabakaran, S. Mohan, Ind. J. Phys. 63B (1989) 468–473.
[44] B. Mikhova, H. Duddeck, ^{13}C-NMR spectroscopy of coumarins and their derivatives: a comprehensive review, in: Atta-ur-Rahman (Ed.), Studies in Natural Product Chemistry, vol. 18, Elsevier Science, Amsterdam, 1996, p. 971.
[45] T. Zolek, K. Paradowska, I. Wawer, Solid State Nucl. Magn. Reson. 23 (2003) 77–87.
[46] K. Pihlaja, E. Kleinpeter, Carbon-13 Chemical Shifts in Structural and Stereo Chemical Analysis, VCH Publishers, Deerfield Beach, FL, 1994.
[47] Y. Erdogdu, M.T. Güllüoğlu, M. Kurt, J. Raman Spectrosc. 40 (2009) 1615–1623.
[48] M.T. Güllüoğlu, Y. Erdogdu, J. Karpagam, N. Sundaraganesan, Ş. Yurdakul, J. Mol. Struct. 990 (2011) 14–20.
[49] D.A. Kleimman, Phys. Rev. 126 (1962) 1977–1979.
[50] S. Chandra, H. Saleem, S. Sebastian, N. Sundaraganesan, Spectrochim. Acta Part A 78 (2011) 1515–1524.
[51] D. Sajan, H.J. Ravindra, Neeraj Misra, I. Hubert Joe, Vib. Spectrosc. 54 (2010) 72–80.
[52] R.G. Parr, R.A. Donnelly, M. Levy, W.E. Palke, J. Chem. Phys. 68 (1978) 3801.
[53] R.G. Parr, R.G. Pearson, J. Am. Chem. Soc. 105 (1983) 7512.
[54] R.G. Parr, L.V. Szentpaly, S. Liu, J. Am. Chem. Soc. 121 (1999) 1922.
[55] X-P Chen, Y-Q. Ding, Q-W. Teng, Chin. J. Chem. Phys. 21 (2008) 105–110.
[56] R.G. Parr, P.K. Chattaraj, J. Am. Chem. Soc. 113 (1991) 1854.
[57] Z. Zhou, R.G. Parr, J. Am. Chem. Soc. 112 (1990) 5720.
[58] L. Pauling, The Nature of The Chemical Bond, third ed., Cornell University, 1960.
[59] W. Kohn, A.D. Becke, R.G. Parr, J. Phys. Chem. 100 (1996) 12974.